Journal of New Technology and Materials
JNTM
Vol. 02, N°01 (2012)30-33

OEB Univ. Publish. Co.

Influence of Optical Kerr Nonlinearity on the Dynamic Behavior of Quantum Cascade Laser

A. Hamadou[a], Jean-Luc Thobel[b] and S. Lamari[c]

[a] *Département ST, Institut des Sciences et de Technologies, Université El Bachir El Ibrahimi, Bordj Bou Arreridj, Algeria*

[b] *Institut d'Electronique, de Microélectronique et de Nanotechnologie (IEMN), UMR 8520, Université Lille 1, Avenue Poincaré, BP 60069, 59652 Villeneuve d'Ascq Cédex, France*

[c] *Département de Physique, Université Ferhat Abbas de Sétif, Algeria*

Received: Feb 21, 2012; revised: June 05, 2012; accepted: June 11, 2012

Abstract

The effect of optical Kerr nonlinearity on the dynamic behaviors of quantum cascade laser operating in the mid-infrared is theoretically studied. Our model is based on three-level rate equations including the dependence of the loss on photon number in the cavity. The optical stability domain that allows for the determination of current injection is investigated. The equation that allow for the determination of the delay time is derived within the premises of our model in the most general case. Furthermore, nonlinear effects influence significantly the dynamics of photons in cavity and electrons in the upper laser level.

Key words *quantum cascade laser; optical Kerr nonlinearity; dynamic behaviours; turn-on delay time; built-up time.*

1. Introduction

Quantum cascade (QC) lasers [1] have gained more and more attention as unique coherent light sources in the mid-infrared. As opposed to conventional ones QC lasers present a fundamental advantage residing in their characteristic property consisting in the control of the wavelength of the emitted light via the layer thickness rather than the band gap. This allows for the emission wavelength of such a laser to be changed at will without resorting to a different semiconductor.

Optical Kerr nonlinearity effects have been studied and developed in intersubband transition in multi-quantum well structures by several authors [2-4]. The effects are due in mid-infrared to the large values of third order nonlinearities near a resonant intersubband transition [5-6]. The QC laser with saturable absorber mechanism due to Kerr effect has also been studied both theoretically and experimentally in recent years by using Maxwell-Bloch equations derived from semiclassical laser treatment when the laser operates in multimode regime [7-8].

In a QC laser the optical Kerr nonlinearity plays an essential role in the behaviour of optical media. A medium with optical Kerr nonlinearity can induce mode locking and thus lead to the generation of short lasers pulses [3]. On the other hand, the QC laser with optical Kerr nonlinearity leads to a photon number dependence of the losses and thus influences the static and dynamic behaviour regime [9]. Therefore, studies of QC laser with optical Kerr nonlinearity are important for potential applications in intersubband photonics field.

Our theoretical treatment laid below focuses only on the electrically injected three-level QC laser design proposed by H. Page [10] where lasing takes place through transitions from the upper state (level 3) to the lower state (level 2), and the latter being subsequently depopulated by longitudinal optical (LO) phonon emission into the ground state (level 1). Intersubband phonon scattering also occurs between levels 3 and 2, and 3 and 1, and is the main competing non-radiative process in mid-infrared QC lasers.

The aim of this work is to present numerically and analytically the effects of optical Kerr nonlinearity on the dynamic behaviours of QC laser operating in a single-mode.

2. Rate equation model

The QC laser rate equations with nonlinear Kerr effect for electron number N_3, N_2, and N_1 in levels 3, 2, and 1, and the photon number N_{ph} in the cavity can be written in the following form [9]:

$$\frac{dN_3}{dt} = WL\frac{J}{e} - \frac{N_3}{\tau_3} - \Gamma\frac{c'\sigma_{32}}{V}(N_3 - N_2)N_{ph}, \quad \text{(1a)}$$

$$\frac{dN_2}{dt} = \frac{N_3}{\tau_{32}} - \frac{N_2}{\tau_{21}} + \Gamma\frac{c'\sigma_{32}}{V}(N_3 - N_2)N_{ph}, \quad \text{(1b)}$$

$$\frac{dN_1}{dt} = \frac{N_3}{\tau_{31}} + \frac{N_2}{\tau_{21}} - \frac{N_1}{\tau_{out}}, \quad \text{(1c)}$$

$$\frac{dN_{ph}}{dt} = N\Gamma\frac{c'\sigma_{32}}{V}(N_3 - N_2)N_{ph} + N\beta\frac{N_3}{\tau_{sp}} - \frac{1}{\tau_p}\left(1-\gamma_0 N_{ph}\right)N_{ph}. \quad \text{(1d)}$$

In the above system of equations, J denotes the electron current density that tunnels into the upper level and e is the electronic charge, while W and L are the lateral dimensions of the cavity, σ_{32} is the stimulated emission cross section between the upper and lower levels. Denoting by N and L_p the number of stages and length of each one of these, the whole volume V of the active area is then given by $NWLL_p$. In addition, in the above equations we introduced the mode confinement factor Γ and the average velocity of light in the system c' given by $c' = c/n_{eff}$ where n_{eff} and c are respectively the effective refractive index of the cavity and the speed of light in vacuum whereas τ_p stands for photon lifetime and is determined by facet loss and waveguide loss of the cavity. The system dynamics is mainly determined by the three non-radiative scattering times denoted by τ_{32}, τ_{31}, and τ_{21} that are due to LO-phonon emission between the corresponding levels as well as by the radiative spontaneous relaxation time τ_{sp} between levels 3 and 2. Furthermore, between two adjacent stages we model the escape of electrons by a rate $1/\tau_{out}$ where τ_{out} stands for the electron escape time. To complete the picture, we take into consideration the proportion of spontaneous emission events that emit a photon into the cavity mode denoted by β [11]. For the sake of convenience, let us also introduce the lifetime τ_3 of the upper level which we write as $\tau_3 = \left(\tau_{32}^{-1} + \tau_{31}^{-1}\right)^{-1}$

The last term in Eq. (1d) models the nonlinear loss, per unit time, in the cavity due to the nonlinearity of the intersubband transition in quantum well. The nonlinear loss coefficient per unit time χ is obtained through the nonlinear refractive index n_2 [3], defined by $n = n_{eff} + n_2 I$ [3], where n is the refractive index, n_2 depends on the optical frequency detuning, and I is the light intensity in the cavity. I is related to the slowly varying envelope of the electric field E by $I = 2n_{eff}\varepsilon_0 cE^2$, where ε_0 is the permittivity of vacuum.

Using the relation between the nonlinear loss coefficient per length and n, $\ell = n/(c\tau_p)$, one easily finds for $n_2 \langle 0$ the relation obtained in literature, $\ell = \ell_0 - \gamma E^2$ [7], where $\ell_0 = n_{eff}/(c\tau_p)$ is the linear loss coefficient per unit length and γ is called "self-amplitude modulation coefficient" [7] and related to the n_2 by $\gamma = 2n_{eff}\varepsilon_0 n_2 / \tau_p$ [9].

Noting that $\chi_0 = c\ell_0 / n_{eff}$ and $\chi = c\ell / n_{eff}$ and using the relation between the electric field and the number of photons $N_{ph} = 2\varepsilon_0 VE^2/(\hbar\omega)$, one easily finds the relation $\chi = \chi_0(1-\gamma_0 N_{ph})$, where

$$\gamma_0 = \frac{c\tau_p \hbar\omega}{2n_{eff}\varepsilon_0 V}\gamma , \qquad (2)$$

is the dimensionless coefficient which characterises the magnitude of nonlinear effects. In our simulations, we will consider γ_0 as the fundamental parameter.

In Eq. (2) $\hbar\omega$ is the photon energy, $\chi_0 = 1/\tau_p$ and the proportionality constant $c\tau_p\hbar\omega/(2n_{eff}\varepsilon_0 V)$ is of the order of 5 V^2/m in the QC laser studied here.

In the following, we use in our calculation the parameters taken from Refs. [10-15]: τ_{21}=0.3ps, τ_{32}=2.1 ps, τ_3=1.4 ps, τ_p=3.36 ps, Γ=0.32, n_{eff}=3.27, N=48, W=34 µm, L=1 mm, L_p=45 nm, β=2×10^{-3}, σ_{32}=1.8×10^{-14} cm^2, and $N_{ph,sat}$= 9.16×10^8.

In Ref. [9] we have found theoretically that the stable solution of photon number is given by

$$N_{ph,stat} = \frac{\left(-\gamma_0 N_{ph,sat} + 1\right)}{2\gamma_0} - \frac{\sqrt{\left(\gamma_0 N_{ph,sat} + 1\right)^2 - 4\gamma_0 N_{ph,sat}\dfrac{J}{J_{th}}}}{2\gamma_0}, \qquad (3)$$

where $N_{ph,sat}$ is the photon saturation number given by [9,12]

$$N_{ph,sat} = \frac{1}{\tau_3(1+\dfrac{\tau_{21}}{\tau_{31}})\Gamma\dfrac{c'\sigma_{32}}{V}}, \qquad (4)$$

and J_{th} denotes the threshold current density and given by [9]

$$J_{th} = \frac{eL_p}{\Gamma c'\sigma_{32}\tau_p\tau_3(1-\dfrac{\tau_{21}}{\tau_{32}})}. \qquad (5)$$

In Eq. (3), the normalized current injection verify the well-known optical stability domain (OSD) condition [9]

$$1 \langle \frac{J}{J_{th}} \langle \frac{1}{2} + \frac{\gamma_0 N_{ph,sat}}{4} + \frac{1}{4\gamma_0 N_{ph,sat}} = \left(\frac{J}{J_{th}}\right)_{\max}, \qquad (6)$$

where the quantity $(J/J_{th})_{\max}$ is the endpoint of OSD. These results agree at least qualitatively with the recent experimental observations reported for 8 µm by Gordon *et al.* [7].

We show in Fig.1 the variation of the endpoint of OSD $(J/J_{th})_{\max}$ as a function of the dimensionless parameter γ_0. It is worthwhile to stress the strong decrease of $(J/J_{th})_{\max}$ as γ_0 increases from its minimal value 5×10^{-11} upward. The physical reason of this result is apparent: large detuning of the QC laser frequency away from resonance leads to high Kerr nonlinearity values, thereby suppressing the OSD to near zero.

In general, the lower the parameter γ_0, the more obvious threshold optical stability behaviour.

From these results it is easy to determine analytically the point where OSD will be lost by setting $(J/J_{th})_{\max} = 1$ in Eq. (6). We have found that the system will lose OSD at $\gamma_0 = 1/N_{ph,sat}$. We can propose a possible experimental test of the effect by measuring the output power as a function of the current for different frequency detuning of the QC laser.

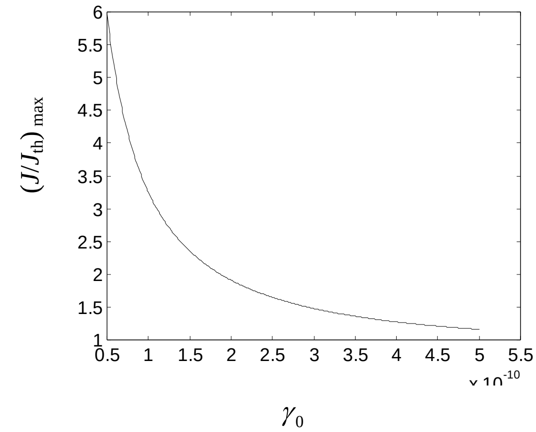

Fig.1. Endpoint of optical stability domain $(J/J_{th})_{max}$ as a function of the dimensionless coefficient γ_0

3. Dynamical behaviours

In the following we explore the temporal evolution of the population of levels N_1, N_2 and N_3, the population inversion ΔN, and the photon number N_{ph} under various values γ_0. We carry this out by solving the system of nonlinear differential equations given in Eqs.(1.a-d) using a 4[th] order Runge-Kutta method with an integration step $h_0 = 0.1$ ps and the following initial conditions $N_1(0) = N_2(0) = N_3(0) = N_{ph}(0) = 0$, the injection current J being finite and above threshold.

In Fig 2 we show the evolution of the electron number in the levels 3, 2, and 1 as a function of time for different values of γ_0, the results are all obtained for an injection current $J = 1.45 J_{th}$. We see that the electrons levels are quickly filled during the initial transient and then their population remains almost constant during a quite long period of time. After about 80 ps the number of electrons in the level 3 (level 2) decreases (increases) before reaching its stationary value depending on the value of γ_0: the higher the parameter γ_0 the lower (higher) the steady state value on level 3 (level 2). The steady state population in level 3 depends strongly on γ_0 as well as in level 2, while the steady state population in level 1 is independent of γ_0.

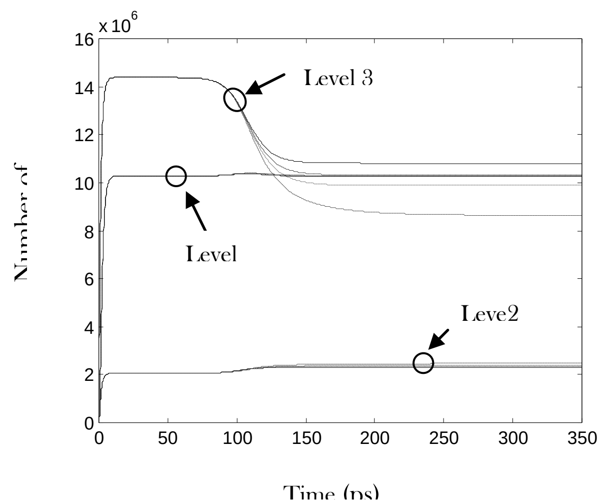

Fig.2. Time evolution of the number of electrons in the levels 3, 2 and, 1 of the QC laser for different values γ_0: Solid line (γ_0=0), dashed line (γ_0=1.25×10^{-10}), dotted line (γ_0=2×10^{-10}), and dash-dotted line (γ_0=3×10^{-10})

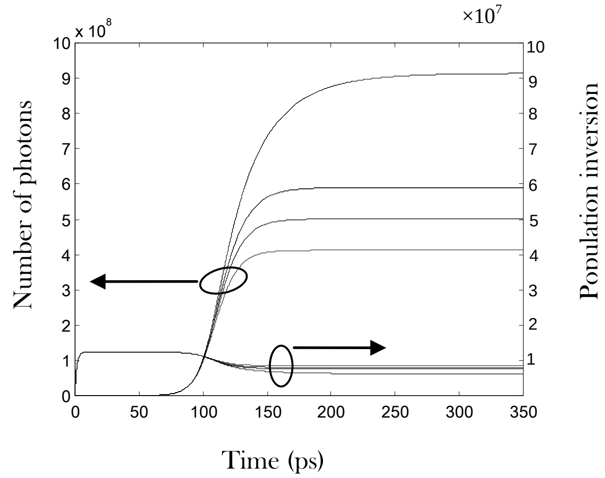

Fig.3. Time evolution of the photon number N_{ph} and population inversion ΔN for different values γ_0: Solid line (γ_0=0), dashed line (γ_0=1.25×10^{-10}), dotted line (γ_0=2×10^{-10}), and dash-dotted line (γ_0=3×10^{-10})

Figure 3 represents the time evolution of the photon number N_{ph} in the cavity. Also shown on the same figure is the population inversion ΔN between levels 3 and 2, the results are all obtained for an injection current $J = 1.45 J_{th}$. We can clearly see that the time needed to establish the stable stationary regime increases with increasing γ_0. As the results the delay time of QC laser increases with increasing of frequency detuning away from resonance.

Now, to compute the delay time t_d that elapses between the moment the bias is applied and the time the photon number reaches 10% of its stationary value we write $t_d \approx t_{th} + \Delta t_{10\%}$, where t_{th} is the turn-on delay time needed for the population inversion to reach its threshold value while $\Delta t_{10\%}$, the built-up time, is the interval of time where the number of photons is still very small. One proceeds in a manner strictly analogous to that of the Ref. [12], one gets

$$t_d \approx t_{th} + \frac{\tau_p}{\sqrt{\Delta}} \ln \frac{\frac{1}{10} N_{ph,stat} + \frac{\left(\frac{J}{J_{th}} - 1\right) - \sqrt{\Delta}}{2\gamma_0}}{\frac{\left(\frac{J}{J_{th}} - 1\right) - \sqrt{\Delta}}{2\gamma_0} + \frac{1}{10} N_{ph,stat} \frac{\left(\frac{J}{J_{th}} - 1\right) - \sqrt{\Delta}}{\left(\frac{J}{J_{th}} - 1\right) + \sqrt{\Delta}}} \qquad (7)$$

where the time t_{th} is solution of the equation [12]

$$\frac{\xi_1\exp(-\frac{t_{th}}{\tau_3})-\xi_2\exp(-\frac{t_{th}}{\tau_{21}})}{\xi_1-\xi_2}=1-\frac{J_{th}}{J}, \tag{8}$$

where the coefficients ξ_1 and ξ_2 are defined as [12]

$$\xi_1=1+\frac{\tau_{21}}{\tau_{32}}\frac{1}{\frac{\tau_{21}}{\tau_3}-1},$$

$$\xi_2=\frac{\tau_{21}}{\tau_{32}}\frac{1}{1-\frac{\tau_3}{\tau_{21}}}, \tag{9}$$

and

$$\Delta=\left(\frac{J}{J_{th}}-1\right)^2-4\gamma_0 WL\frac{J}{e}\tau_3\tau_p\frac{N\beta}{\tau_{sp}}. \tag{10}$$

We show in Fig.4 the variation of the Built-up time as a function of the dimensionless coefficient γ_0 for normalized current density $J=1.45J_{th}$. It is found that Built-up time is an increasing function of γ_0.

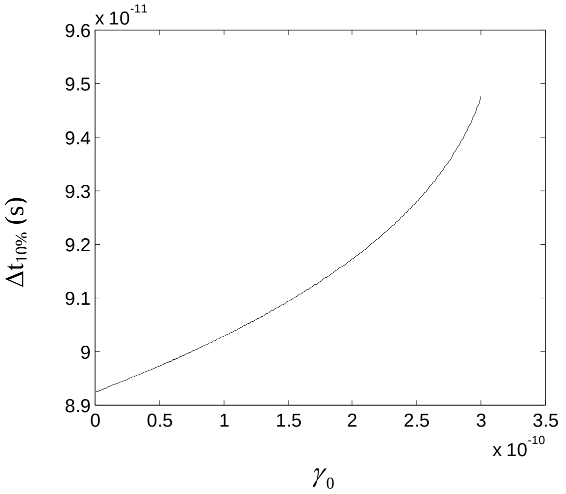

Fig.4. Built-up time variation versus coefficient γ_0

4. Conclusion

In summary, by using a simple rate equation model, we have investigated numerically and analytically the dynamic behaviours of a three-level mid-infrared QC laser in presence of optical Kerr nonlinearity. We have defined a dimensionless parameter γ_0, which characterises the magnitude of nonlinear effects. We have demonstrated that γ_0 can affect the optical stability domain dramatically. Numerical results show that the dynamic transient of electron in the upper laser level and photon in the cavity can be greatly modified by varying γ_0. We also developed an analytical scheme to derive the delay time as functions of γ_0, J and the different scattering times of the system.

Acknowledgments
The authors are much indebted to Dr. F. Dessenne from IEMN, University Lille 1, for his generous help.

References

[1] J. Faist, F. Capasso, D. L. Sivco, C. Sirtori, A. L. Hutchinson, A. Y. Cho, Science 264 (1994) 553-556.
[2] F. Capasso, C. Sirtori, A. Y. Cho, IEEE J. Quantum Electron 30 (1994) 1313-1326.
[3] R. Paiella, F. Capasso, C. Gmachl, D. L. Sivco, J. N. Baillargeon, A. L. Hutchinson, A. Y. Cho, H. C. Liu, Science 290 (2000) 1739-1742.
[4 J. Bai, D. S. Citrin, J. App. Phys 106 (2009) 031101-14.
[5] C. Sirtori, F. Capasso, D. L. Sivco, A. Y. Cho, Phys. Rev. Lett 68 (1992) 1010-1013.
[6] J. Bai, D. S. Citrin, IEEE J. Quantum Electron 43 (2007) 391-398.
[7] A. Gordon, C. Y. Wang, L. Diehl, F. X. Kärtner, A. Belyanin, D. Bour, S. Corzine, G. Höfler, H. C. Liu, H. Schneider, T. Maier, M. Troccoli, J. Faist, F. Capasso, Phys. Rev. A 77 (2008) 053804-18.
[8] A. Soibel, F. Capasso, C. Gmachl, M. L. Peabody, A. M. Sergent, R. Paiella, H. Y. Hwang, D. L. Sivco, A. Y. Cho, H. C. Liu, C. Jirauschek, F. X. Kärtner, IEEE J. Quantum Electron 40 (2004) 844-851.
[9] A. Hamadou, J.-L. Thobel, Opt. Commun 284 (2011) 2972-2979.
[10] H. Page, C. Becker, A. Robertson, G. Glastre, V. Ortiz, C. Sirtori, Appl. Phys. Lett 78 (2001) 3529-3531.
[11] M. Yamanishi, T. Edamura, K. Fujita, N. Akikusa, H. Kan, IEEE J. Quantum. Electron 44 (2008) 12-29.
[12] A. Hamadou, S. Lamari, J.-L. Thobel, J. App. Phys 105 (2009) 093116-6.
[13] A. Hamadou, J.-L. Thobel, S. Lamari, Opt. Commun 281 (2008) 5385-5388.
[14] S. Hofling, R. Kallweit, J. Seufert, J. Koeth, J.P. Reithmaier, A. Forchel, J. Cryst. Growth 278 (2005) 775-779.
[15] R. C. Iotti, F. Rossi, Rep. Prog. Phys 68 (2005) 2533-2571.